

Modelling the Single-Lane Change Maneuver of Nonlinear 7 DOF 4-Wheel Steering Vehicle for a Passenger Car

Hussein Awad Kurdi Saad ^{a,b}, Ahmed Hammodi Ali ^a, and Ahmed Salim Naser Al-murshedi ^{a a}
 Engineering Technical College of Al-Najaf, Al-Furat Al-Awsat Technical University (ATU), Najaf, Iraq,
^bEmbry-Riddle Aeronautical University, Florida, USA 32114,

Abstract - This work emphasis on simulating the single-lane change maneuver. It is based on the Seven Degree of Freedom (7 DOF) 4-wheel steering vehicle model in absence of longitudinal tractive or braking forces. The improvements such as vehicle center gravity's XY position in inertial, or terrain-fixed reference frame, time of body-fixed velocities in two dimensions, and angular velocities have been achieved. A 2016 Toyota Avalon, XLE Premium, had been used as a case study to simulate vehicle model. All four tire's slip angle, normal forces, and angular velocities with understeering case (U.S. case) have been adopted. The 7 DOF 4-wheel model was performed by utilizing from the framework supplied by the motorist inputs to the location and velocity kinematics with creation of the forces and moment for solving 2D dynamics formulations of motion. Furthermore, a constant steering maneuver with a steering input is simulated. The single lane change maneuver is simulated with initial velocity of 60 mph (26.82 m/s).

Keywords: Modelling, Single-lane maneuver, Nonlinear 7 DOF, 4-wheel steering vehicle model, Under-steer case (US case).

Introduction - Lane-change is considered as one of the most significant techniques for automobiles. It possesses a magnificent effect on traffic issues. Utilizing intelligent leading technologies to enhance traffic safety and efficiency could be substantially done by automated lane change. Many previous studies were concentrated on the independent lane-change relied on two-lane without collaboration. These investigations have focused on the path and accomplished perfect outcomes. Bezier curve and quantic polynomial trajectories were mostly utilized in path planning [1]. Tian, et al comprehended the 4-wheel variance steering function of an "In-wheel Motor" (IWM) motivated through an electric automobile with a system of steer-by-wire. They estimated fractional and decoupling regulators for the 4WSV to gain the standard inputs and also implement steering angles for the front and rear wheels [2]. Ivanov et al worked on motorized control systems as apparatuses of the integrated motion control. They attempted to enhance an automobile implementation in relative to lateral, longitudinal, and vertical locomotion kinematics through an assistance of several powertrain and chassis systems [3]. Mahjan et al searched mainly innovative techniques like linked and autonomous automobiles that are quick being an actuality. Providing data to vehicles and drivers is crucial approach for preventing traffic accidents [4]. Ahmed et al introduced lane-changes that could be obligatory relied on how the car's operator realizes conditions on both the target and present lanes. In addition to these conditions, environmental situations which impact the determination to change lanes [5]. The objected automotive speed through lane changing ordinarily raises, and troubles in the adjacent lane may be monitored since the maneuver of lane-changing was aggressive [6]. Motorists who are interacting for a lanechange should be attentive and cautioned to treat these troubles and become safe lane changing. However, this case is not always happened: it has revealed that 44 percent of implemented lane changes was used for turning indicators [7]. Zhang et al analyzed a preview of a single-point track algorithm scheme that can be carried out to a great curvature pathway, which can direct the automotive to track an arc-path with huge curvature, under an evidence of guaranteeing a real-time benefit of the preview of single-point. The tracking algorithm that had been proposed can be applied to an armed unmanned automotive throughout using a GPS navigation. The best preview point is gained based on data points of variance GPS indication. The perfect tracking algorithm was utilized to estimate the request navigation angle, and an altering universe fuzzy sliding method controller (FSMC) was planned to regulate the automotive lateral movement and more precise motion responses, that was verified through the combined CarSim and a simulation design of Simulink, under several working circumstances. The researches adopted an actual truck via utilizing an Autobox platform to make a verification. The consequences display that the control lateral motion of pathway tracking planned can attain an precise and operative control influence, and had real-time behavior for implementation of engineering [8]. Asiabar et al invented an algorithm of a higher and a lower-level controller that was described a direct yaw moment control. The algorithm can lead to the corrective yaw moment via straight regulator of braking torques and driving of 4 in-wheel brushless direct existing motors positioned at the vacant space of automobile wheels. The offered control system can work to retain longitudinal speed constant in maneuvers. Also, they were created sliding mode governor

to produce the rectifying yaw moment such that the yaw rate tracks the desired value and the vehicle sideslip angle maintains limited so as to improve vehicle handling stability [9]. Jianyong et al introduced a novel automobile combined robust model matching governors, that conjoins straight yaw moment control and 4 wheels steering. The study aimed to develop the automotive treatment stability and efficiency. Their model grounded on matrix of linear inequalities. Their investigations advanced in the model a sliding mode observer through using a

vehicle yaw rate to find out a measurement for a sideslip angle of an automobile which is challenging to accomplish in practice [10]. Therefore, the purpose of this study is to simulate the single-lane change maneuver with initial velocity of 60 mph and no longitudinal tractive or braking forces. Vehicle center gravity's XY position in inertial, or terrain-fixed reference frame, and time of body-fixed velocities in two dimensions will be simulated. Moreover, all four tire's slip angle, normal forces, and angular velocities will be displayed with U.S. case. To illustrate, a 2016 Toyota Avalon, XLE Premium, is used as a case study in this paper to simulate vehicle model.

TABLE 1
Vehicle parameters used for a 2016 Toyota Avalon, XLE Premium [11][15]

parameters	values
Wheelbase length (L)	2.819 m
Track width	1.585 m
Vehicle weight	1570 kg
Mass moment of inertia, z-axis, I_z	1369 kg-m ²
U.S. front/rear weight ratio	38/62
Center of gravity height (L/5)	0.5638 m
A single tire's inertia, I_y	1.3 kg-m ²
Rolling resistance loss coefficient	2% of loss torque
Rolling radius of r_{tire}	0.323 m
Lateral tire stiffness c_a	76,459 N/rad
Body-fixed velocity: v_x	13.4 m/s
Steering input δ	0.095 rad
the Newton-Euler block using stepsize	$h=0.001$ (s)
Time step	[0 16] sec
The instantaneous turn radius (R)	28.95 m
Density of air ρ	1.225 kg/m ³
Friction coefficient (C_d)	0.29
Frontal-sectional area (A_f)	2.584 m ²

MOTION EQUATION OF 7-DOF MODEL

This study indicates the schematic below which is initiated by the motorists inputs like throttle, brake, gear, and steering traces. Then, the position and velocity kinematics are calculated. In addition, sum forces and moments are computed in the model. Furthermore, 2D dynamics equations of motion are applied. Finally, the model outputs of the vehicle are performed by visualization.

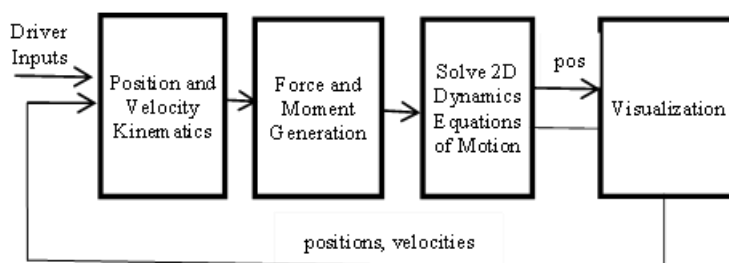


FIGURE 1
The 2D, 7DOF Model Subsystems

FREE BODY DIAGRAM (FBD) OF 4-TIRE VEHICLE MODEL

Each tire generates forces in x & y directions (F_x and F_y) in the steered tire frame. Also, one approach would be writing xy components of steered tire.

$$\uparrow \Sigma F_x = F_{x,f} \cdot \cos \delta - F_{y,f} \cdot \sin \delta + F_{x,r} = m a_x \dots (1)$$

$$\rightarrow \Sigma F_y = F_{x,f} \cdot \sin \delta - F_{y,f} \cdot \cos \delta + F_{y,r} = m a_y \dots (2)$$

$$M_g = [F_{x,f} \cdot \sin \delta - F_{y,f} \cdot \cos \delta] \cdot a - F_{y,r} \cdot b = I_{zz} \cdot \dot{\omega}_a \dots (3)$$

A rotation matrix is developed to transform the tire forces in steered tire frame, xy, into the body-fixed xy frame.

$$\begin{bmatrix} i \\ j \end{bmatrix} \begin{bmatrix} \cos \delta & \sin \delta \\ -\sin \delta & \cos \delta \end{bmatrix} \begin{bmatrix} I \\ J \end{bmatrix} \dots \dots \dots (4)$$

So, the inertial or terrain frame XY is computed by this equation:

$$\begin{bmatrix} I \\ J \end{bmatrix} = \begin{bmatrix} \cos \delta & -\sin \delta \\ \sin \delta & \cos \delta \end{bmatrix}^T \begin{bmatrix} i \\ j \end{bmatrix} \dots \dots \dots (5)$$

To get position in XY coordinates, velocity of XY should be integrated:

$$\vec{v}^{XY} = [T^T(\delta)] \cdot \vec{v}^{xy} \dots \dots \dots (6)$$

$$X = \int v_X \cdot dt \dots \dots \dots (7)$$

$$Y = \int v_Y \cdot dt \dots \dots \dots (8)$$

A simple rotational subsystem is formed as the following equation:

$$M_A = \tau_A - \tau_{loss} - T_{tension} = I_a \cdot \dot{\omega}_a \dots \dots \dots (9)$$

Where τ_A : Positive axle tractive from drivetrain

τ_{loss} : Bearing loss

The tension torque is computed by this formula:

$$T_{tension} = F_x \cdot R_{tire} \dots \dots \dots (10)$$

The tractive effort is calculated as the following equation [12].

$$F_x = m \cdot a_x + \mu_{rr} m \cdot g + \frac{1}{2} \rho \cdot c_d \cdot A_f \cdot V^2 + m \cdot g \sin \theta \dots \dots \dots (11)$$

Each tire is steered at angle δ_i with respect chassis:

$$\tan(\delta_i - \alpha_i) = \frac{V_{yi}}{V_{xi}} \dots \dots \dots (12)$$

Starting with longitudinal weight transfer, the first step is applying a simple FBD with Newton's second law. Also, sum moments about the rear contact patch, and then sum moments about the front contact patch of the vehicle are applied. In addition, the other process is to move to lateral weight transfer. A simple FBD lateral forces are demonstrated. Also, sum moments of center gravity (CG) and left normal force are solved, and then right normal is solved too. The essential concept of Ackerman steering consists of rotating the inner wheel a little sharper than the outer wheel to decrease tire slip angle. With the track width (w) which is considered as the lateral wheel separation, the wheelbase (L) which is considered as the longitudinal wheel separation, δ_i the relative steering angle of the inner wheel, δ_o the relative steering angle of the outer wheel and (R) the distance between ICR (instantaneous center of rotation) and the center of the vehicle. Figure (2) shows the Ackermann steering [14][18].

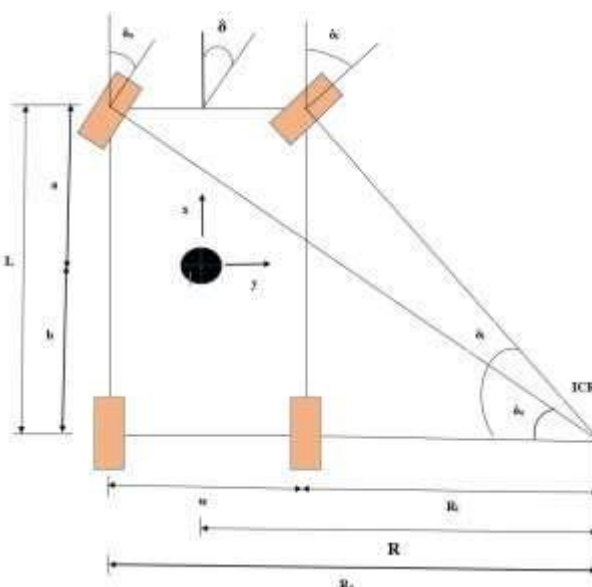


FIGURE 2
Ackermann steering system

The Ackerman steering equation could be derived totally readily by considering the three triangles founded by:

$$\tan(\delta_o) = \frac{L}{R_o} \dots \dots \dots \quad (13)$$

$$\tan(\delta_i) = \frac{L}{R_i} \dots \dots \dots \quad (14)$$

So, the system could be assumed as a Bicycle model used in this steering angle related to Ackermann steering system.

$$\tan(\delta) = \frac{L}{R} \dots \dots \dots \quad (15)$$

This system is linearized, and the equation could be written in the following form:

$$\delta \approx \frac{L}{R} \dots \dots \dots \quad (16)$$

Where δ : steering angle.

R: radius about the vehicle steers.

L : wheelbase length.

A Ratiometric method for normal force estimates is used in the following [14][17]: Figure (2) also indicated the dimensions of steering system.

Front left normal force is expressed as:

$$N_{FL} = \left[\frac{b}{L} - \left(\frac{h}{L} \right) \left(\frac{a_x}{q} \right) \right] \cdot \left[\left(\frac{d}{w} \right) + \left(\frac{h}{w} \right) \left(\frac{a_y}{q} \right) \right] \cdot W \quad \dots (17)$$

Front right normal force is computed by this formula:

$$N_{FR} = \left[\frac{b}{L} - \left(\frac{h}{L} \right) \left(\frac{a_x}{q} \right) \right] \cdot \left[\left(\frac{c}{w} \right) - \left(\frac{h}{w} \right) \left(\frac{a_y}{q} \right) \right] \cdot W \dots (18)$$

Right left normal force is determined by this equation:

$$N_{RL} = \left[\frac{a}{L} + \left(\frac{h}{L} \right) \left(\frac{a_x}{q} \right) \right] \cdot \left[\left(\frac{d}{W} \right) + \left(\frac{h}{W} \right) \left(\frac{a_y}{q} \right) \right] \cdot W \dots (19)$$

Rear right normal force is indicated as:

$$N_{RR} = \left[\frac{a}{L} + \left(\frac{h}{L} \right) \left(\frac{a_x}{q} \right) \right] \cdot \left[\left(\frac{c}{w} \right) - \left(\frac{h}{w} \right) \left(\frac{a_y}{q} \right) \right] \cdot W \dots (20)$$

Each tire can experience longitudinal slip ration, SR_i , and slip angle, α_i . To illustrate, the velocity of front left tire is expressed as the following equation below, and the same processes for the other tires are indicated.

$$\vec{V}_{FL} = \begin{bmatrix} V_x \\ V_y \\ 0 \end{bmatrix} + \begin{bmatrix} i & j & k \\ 0 & 0 & \phi \\ +a & -c & 0 \end{bmatrix} = \begin{bmatrix} V_x + c\phi \\ V_y + a\phi \\ 0 \end{bmatrix} \dots (21)$$

A simple free-body diagram (FBD) of a tire experiencing pure longitudinal slip. Slip ratio equation could be demonstrated as:

$$SR = \frac{R_{tire} \cdot \omega_{tire} - V_x}{V_x} \dots \dots \dots (22)$$

Lateral velocity for front left tire.

$$\begin{bmatrix} V_{FL,xs} \\ V_{FL,ys} \end{bmatrix} = \begin{bmatrix} \cos \delta & \sin \delta \\ -\sin \delta & \cos \delta \end{bmatrix} \cdot \begin{bmatrix} V_{FL,x} \\ V_{FL,y} \end{bmatrix} \dots \dots \quad (23)$$

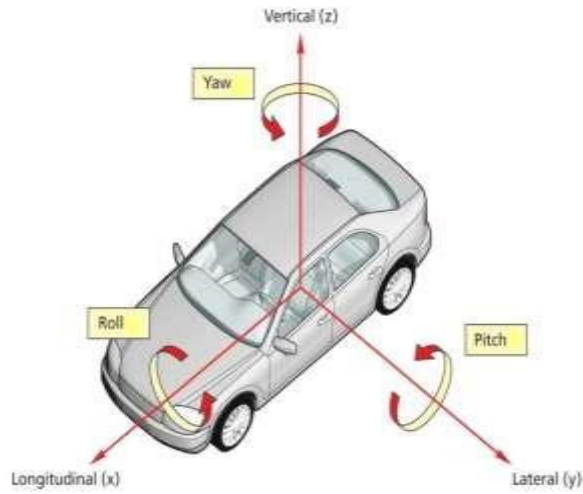


FIGURE 3
Vehicle coordinate system and notation [13]

Rolling resistance loss torque indicates as a function of variable normal force,

$$T_{loss} = r_{tire} \cdot (\mu_{rr} \cdot F_{z,i}) \dots \dots (24)$$

Nonlinearities are implemented for steering,

$$T_i(\delta_i) = \begin{bmatrix} \cos(\delta_i) & -\sin(\delta_i) \\ +\sin(\delta_i) & \cos(\delta_i) \end{bmatrix} \dots \dots (25)$$

This study has been dealt with nonlinear version estimated as $c \neq 0$, and $d \neq 0$. Also, variable speed for nonlinear version is $\dot{v}_x \neq 0$.

METHODOLOGY

After building up all the theoretical equations of this model, modelling the Single-Lane change maneuver of nonlinear 7 DOF 4-Wheel Steering Vehicle is applied by using one of the simulating programs like Simulink in MATLAB [16]. To illustrate, the model is performed by computing the alphas calculation, and implementing Pacejka with some forces and moments. Then, the normal forces for all tires are executed. Finally, 2D planer body-fixed dynamics is implemented. Figure (4) shows the overall Simulink code for the vehicle used.

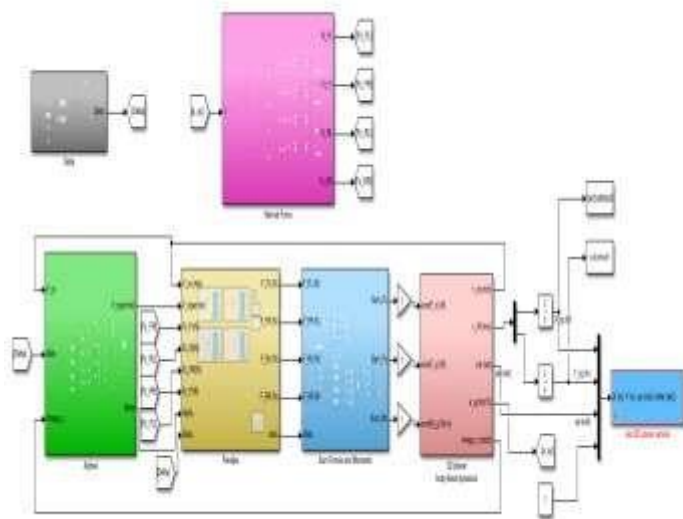


FIGURE 4
Overall Simulink code

For example, the subsystem of the calculation called alpha (slip angle) was indicated in figure (5), and this figure represented all steps how the calculation was done in this model based on the rotational subsystem of all four tires. The slip angles of each tire were gotten by providing the velocity and angular velocity, and rotational subsystems for front left, front right, rear left, and rear right tires as inputs to these computations based on theoretical calculations.

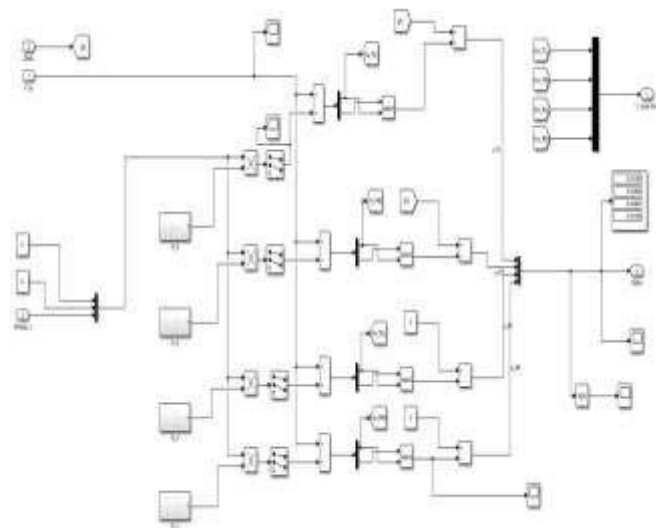


FIGURE 5
Alpha calculations

A simple rotational subsystem was represented a simple FBD of a tire experiencing pure longitudinal slip. Figure (6) represents the rotational subsystem of one tire based on the torque, and some forces inputs of rotational motion of a rigid body in Body-Fixed Coordinates to get the angular velocity of each tire.

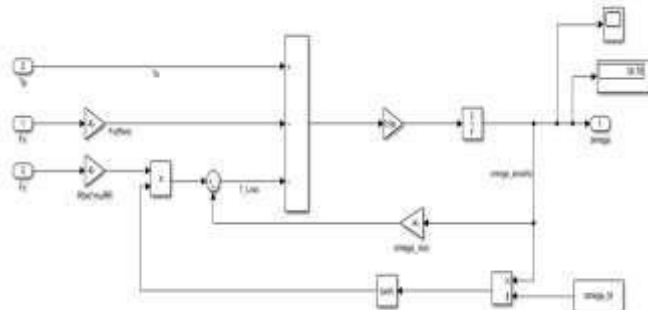


FIGURE 6
Rotational subsystem

The normal forces like front left, front right, right left, and rear right were represented according to the equations (13), (14), (15), and (16) respectively. After creating the ratio for each tire, the normal force has been got according to the estimation for each tire as a function of simple geometry (L, w) and directly measurable signals a_x, a_y . The modelling of these normal forces was implemented simultaneously by these accelerations as inputs with respect all the dimensions, the total weight of the vehicle, and the lateral weight transfer.

RESULTS

The plots are shown in this paper based on the single lane change for under-steer case. Figure (7) displays the simulation of the automobile center gravity's XY position in terrain-fixed reference frame with lane change for US case. The distances were X and Y coordinates in meter (m), and the vehicle travelled from 0 to 220 m in X plane based on (Society of Automotive Engineers) SAE coordinates.

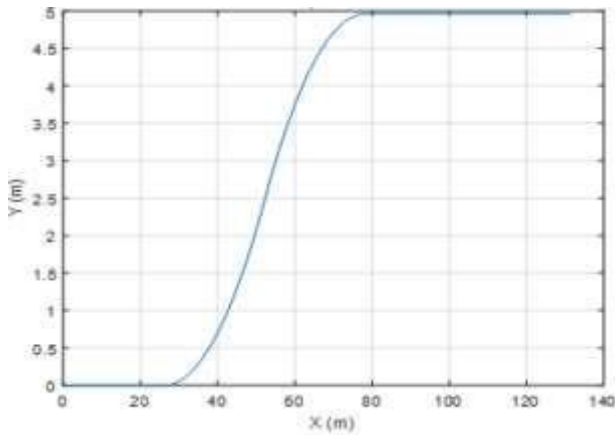


FIGURE 7
Vehicle center gravity's XY position (m) in terrain-fixed reference frame.

Figure (8) shows body-fixed velocity ($V_x=60$ mph), Pacejka tires, under-steer case based on axles torque ($T_{\text{axles}}=0$).

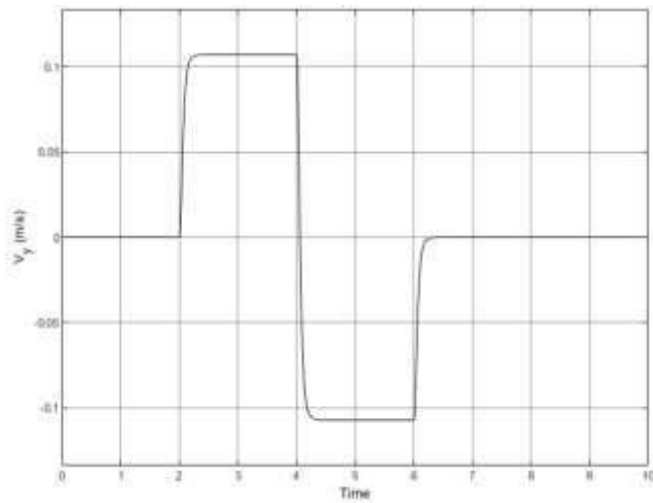


FIGURE 8
Time history (sec) of body-fixed velocity in y-direction (V_y)(m/s).

The slip angles (alpha) are represented in figure (9) with variable normal forces, Pacejka tires, under-steer case based on axles torque ($T_{\text{axles}}=0$). The values of the slip angles for the four tires were (0.03195, 0.02848, 0.02991, and 0.03156) rad.

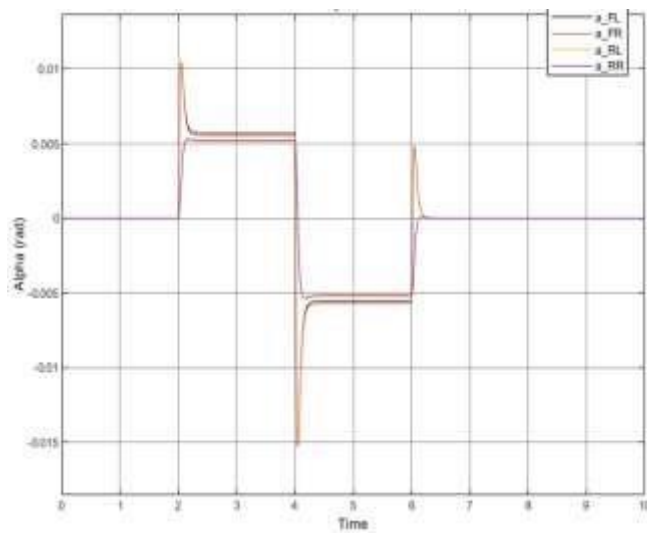


FIGURE 9
Time history (sec) of all four tire's slip angle (rad).

Figure (10) presents the normal forces for each tire like front left (FL), front right (FR), rear left (RL), and rear right (RR), and the variable normal force is considered as a function of (a, b), (c, d), and a_x and a_y . The values of the normal forces were (2927, 2926, 4776, and 4773) N for FL, FR, RL, and RR respectively with the time of 7 seconds.

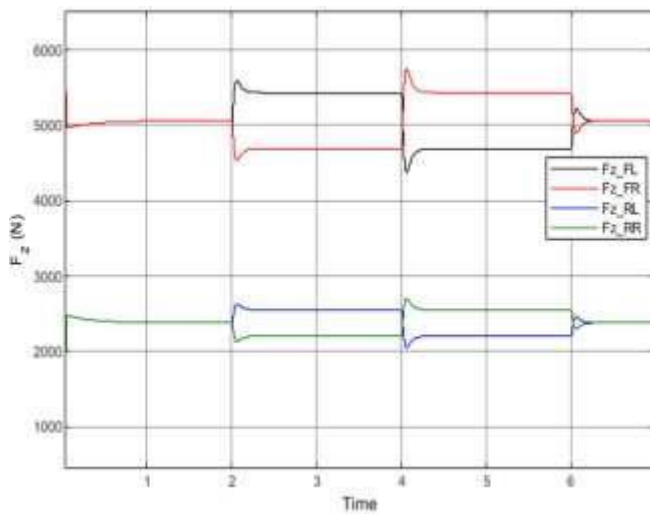


FIGURE 10
Time history (sec) of all four tires normal forces, in Newtons.

Tire forces can be expressed in the tire frame and transformed into body-fixed xy frame from free body diagram of four-tire vehicle model. Each tire generates force in x -direction (F_x) (N). Figure (11) time history of all four tires' traction forces for the vehicle indicated by computing for each tire between -100 to 600 N vs the time through 10 seconds.

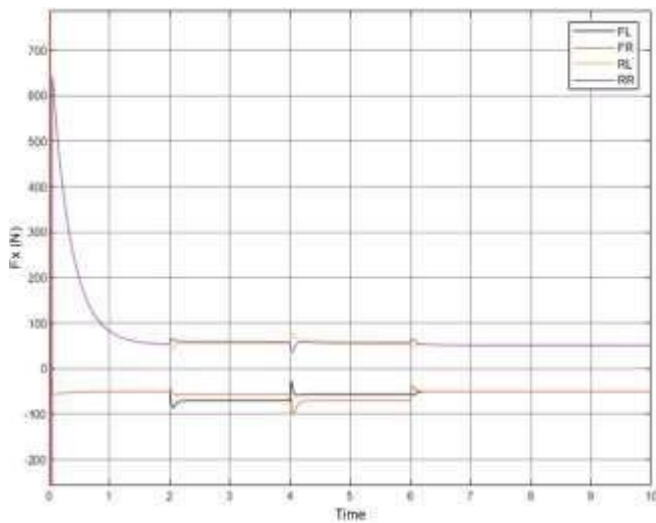


FIGURE 11
Time history (sec) of the force in x -direction (N) vs time (sec).

Figure (12) indicates rate of turning of the angular velocities (ω) of the four tires with variable normal forces, Pacejka tires, understeer case based on axles torque ($T_{\text{axles}} = 0$). The angular velocities of the four tires range from 33.5 to 34.5 (rad/sec) with time of 7 seconds.

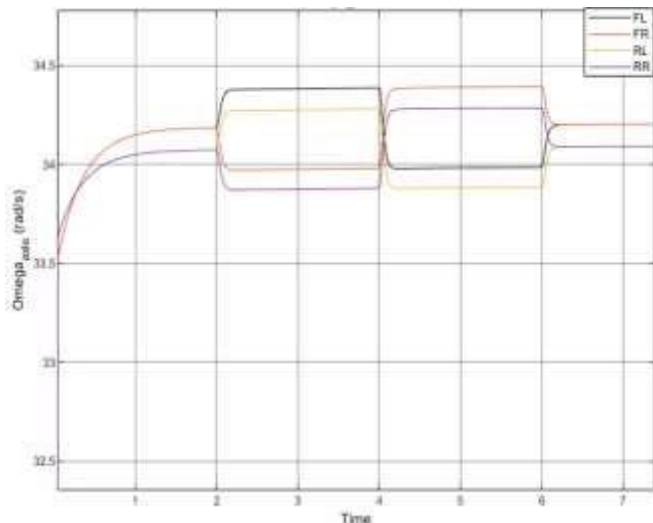


FIGURE 12
Time history (sec) of all four tires angular velocities in (rad/s).

CONCLUSION

In this study, the 7 DOF 4-wheel model was performed theoretically and numerically with under-steer case by utilizing from the framework supplied by the motorist inputs to the location and velocity kinematics with creation of the forces and moment for solving 2D dynamics formulations of motion. The single-lane maneuver of the vehicle was calculated and implemented with the initial velocity of 96.65 Km/h. The distance of the vehicle travelled was 220 m in X-plane coordinate, and the axle torque was 0 N.m. The slip angles were calculated to be performed numerically for the four tires were from 0.02845 rad (1.63°) to 0.03195 rad (1.83°). The normal forces for all tires were implemented to be from 2927 N to 4776 N. The angular velocities were between 33.5 and 34.5 rad/s with 7 seconds period of time. This work is considered as a case study of the 2016 Toyota Corolla which could be applied for the modern conventional and hybrid models of each kind of the automobiles, and the outcomes could be earned based on different characteristics of each model to improve the vehicle movement behavior with the lane change maneuver.

REFERENCES

- [1] Luo, Yugong, et al. "Automotive Innovation." Cooperative Lane-Change Maneuver for Multiple Automated Vehicles on a Highway, Springer, Page 157, 10 Sept. 2019, link.springer.com/content/pdf/10.1007/s42154-019-00073-1.pdf.
- [2] Tian, Jie, Jie Ding, Chuntao Zhang, and Shi Luo. "Four-Wheel Differential Steering Control of IWM Driven EVs." IEEE Access 8 (2020): 152963-152974.
- [3] Ivanov, Valentin, and Dzmitry Savitski. "Systematization of integrated motion control of ground vehicles." IEEE Access 3 (2015): 2080-2099.
- [4] Mahajan V, Katrakazas C, Antoniou C. Prediction of Lane-Changing Maneuvers with Automatic Labeling and Deep Learning. Transportation Research Record. 2020;2674(7):336-347. doi:10.1177/0361198120922210.
- [5] Ahmed, K. I. Modeling Drivers' Acceleration and Lane Changing Behavior. PhD dissertation. Massachusetts Institute of Technology, 1999, p. 189.
- [6] Ioannou, P. A., Stefanovic, M. Evaluation of ACC Vehicles in Mixed Traffic: Lane Change Effects and Sensitivity Analysis. IEEE Transactions on Intelligent Transportation Systems, Vol. 6, No. 1, 2005, pp. 79–89. <https://doi.org/10.1109/TITS.2005.844226>.
- [7] Lee, S. E., Olsen, E. C. B., Wierwille, W. W. A Comprehensive Examination of Naturalistic Lane-Changes. No. DOT HS 809 702. National Highway Traffic Safety Administration, Washington, D.C., 2004.
- [8] Zhang, H.; Yang, X.; Liang, J.; Xu, X.; Sun, X. GPS Path Tracking Control of Military Unmanned Vehicle Based on Preview Variable Universe Fuzzy Sliding Mode Control. Machines 2021, 9, 304. <https://doi.org/10.3390/machines9120304>.
- [9] Asiabar, Aria Noori, and Reza Kazemi. "A direct yaw moment controller for a four in-wheel motor drive electric vehicle using adaptive sliding mode control." Proceedings of the institution of mechanical engineers, part K: journal of multi-body dynamics 233, no. 3 (2019): 549-567.
- [10] Jianyong, Wu, Tang Houjun, Li Shaoyuan, and Fang Wan. "Improvement of vehicle handling and stability by integrated control of four-wheel steering and direct yaw moment." In 2007 Chinese Control Conference, pp. 730-735. IEEE, 2007.
- [11] CarBuzz. "2016 Toyota Avalon XLE Premium Full Specs, Features and Price." CarBuzz, 2016, carbuzz.com/cars/toyota/avalon/2016-toyota-avalon-xle-premium.

- [12] Saad, Hussein A. K. "Enhancing the Fuel Economy of a Plug-in Series Hybrid Vehicle System." *Mechanics and Mechanical Engineering*, Sciendo, Page 131, Vol. 23, No. 1, 2019.
- [13] "AUSTRALASIAN NEW CAR ASSESSMENT PROGRAM (ANCAP) Safety." ANCAP Test Protocol, Lane Support Systems v2.0.2, Coordinate System and Notation, Page 2, 2019.
- [14] Pacejka, Hans B. "Tire and Vehicle Dynamics." ISBNL 978–0-08-097016-5, Elsevier and distributed in conjunction with SAE International., 2012, assets.erau.edu/federror/index.html?docID=892225.
- [15] Baker, Chris, et al. "Aerodynamic Drag - an Overview | ScienceDirect Topics." Train Aerodynamics Fundamentals and Applications, Chapter 7 - Aerodynamic Drag, 2019.
- [16] Furlan, Marco. "MFeval." MFeval - File Exchange - MATLAB Central, 12 Mar. 2021, www.mathworks.com/matlabcentral/fileexchange/63618-mfeval.
- [17] Rajamani, Rejesh. Vehicle Dynamics and Control, Chapter 8, Electronic Stability Control, Pages 201-213, Second Edition, e-book, Springer, 2012.
- [18] Eisele, Robert. "Ackerman Steering." Computer Science & Machine Learning, 2021, www.xarg.org/book/kinematics/ackerman-steering.